

# Sorting Mechanisms Regulating Membrane Protein Traffic in the Apical Transcytotic Pathway of Polarized MDCK Cells

A. Gibson,\* C.E. Futter,\* S. Maxwell,\* E.H. Allchin,\* M. Shipman,\* J.-P. Kraehenbuhl,‡ D. Domingo,§ G. Odorizzi,§ I.S. Trowbridge,§ and C.R. Hopkins\*

\*Medical Research Council Laboratory for Molecular Cell Biology, University College London, WC1E 6BT London, United Kingdom; ‡Swiss Institute for Experimental Cancer Research and Institute for Biochemistry, University of Lausanne, CH-1066 Epalinges, Switzerland; and §Department of Cancer Biology, The Salk Institute for Biological Studies, San Diego, California, 92186-5800

**Abstract.** The transcytotic pathway followed by the polymeric IgA receptor (pIgR) carrying its bound ligand (dIgA) from the basolateral to the apical surface of polarized MDCK cells has been mapped using morphological tracers. At 20°C dIgA-pIgR internalize to interconnected groups of vacuoles and tubules that comprise the endosomal compartment and in which they codistribute with internalized transferrin receptors (TR) and epidermal growth factor receptors (EGFR). Upon transfer to 37°C the endosome vacuoles develop long tubules that give rise to a distinctive population of 100-nm-diam cup-shaped vesicles containing pIgR. At the same time, the endosome gives rise to multivesicular endosomes (MVB) enriched in EGFR and to 60-nm-diam basolateral vesicles. The cup-shaped vesicles carry the dIgA/pIgR complexes to the apical surface where they exocytose.

Using video microscopy and correlative electron microscopy to study cells grown thin and flat we show that endosome vacuoles tubulate in response to dIgA/pIgR

but that the tubules contain TR as well as pIgR. However, we show that TR are removed from these dIgA-induced tubules via clathrin-coated buds and, as a result, the cup-shaped vesicles to which the tubules give rise become enriched in dIgA/pIgR.

Taken together with the published information available on pIgR trafficking signals, our observations suggest that the steady-state concentrations of TR and unoccupied pIgR on the basolateral surface of polarized MDCK cells are maintained by a signal-dependent, clathrin-based sorting mechanism that operates along the length of the transcytotic pathway. We propose that the differential sorting of occupied receptors within the MDCK endosome is achieved by this clathrin-based mechanism continuously retrieving receptors like TR from the pathways that deliver pIgR to the apical surface and EGFR to the lysosome.

**Key words:** transcytosis • polymeric Ig receptor • polarity • MDCK • endosome

**T**HE epithelial monolayers that line the ducts and cavities of the body function as continuous cellular barriers but an extensive membrane protein traffic operates between their luminal and abluminal surfaces. This transcellular transport, generally known as transcytosis (Schaefer et al., 1991; Sztul et al., 1991; Rodriguez-Boulan et al., 1992) is mediated by trafficking receptors whose steady-state distributions on these separate surfaces are closely regulated. Transcytosis has been most thoroughly studied in MDCK cells which, when cultured appropriately, form polarized monolayers and, when induced to ex-

press receptors for the polymeric immunoglobulin receptor (pIgR),<sup>1</sup> transport-bound dimeric IgA ligand (dIgA) from their basolateral to their apical surfaces (Mostov and Simister, 1985; Breitfeld et al., 1989). Modifying pIgR by mutagenesis has shown that its cytoplasmic domain bears a series of trafficking signals which are recognized by sorting mechanisms distributed along the transcytotic pathway (Mostov et al., 1992; Casanova et al., 1990, 1991; Aroeti et al., 1993).

The pathway taken by transcytosing pIgR to the apical

Address all correspondence to C.R. Hopkins, Medical Research Council Laboratory for Molecular Cell Biology, University College London, Gower Street, London WC1E 6BT, UK. Tel./Fax: (44) 171-380-7804. E-mail: c.hopkins@ucl.ac.uk

1. *Abbreviations used in this paper:* AP, adaptor complexes; dIgA, dimeric immunoglobulin A; EGF, epidermal growth factor; EGFR, epidermal growth factor receptor; HRP, horseradish peroxidase; MBV, multivesicular body; pIgR, polymeric immunoglobulin receptor; Tf, transferrin; TR, transferrin receptor; TX100, Triton X-100.

surface has been partly outlined and it is known that pIgR tracers internalize from the basolateral surface into an endosome compartment that contains internalized transferrin receptors (TR) (Barroso and Sztul, 1994; Apodaca et al., 1994). However, while the pIgR are routed apically from this compartment, TR are returned preferentially to the basolateral surface. In unpolarized cells, TR-containing endosome vacuoles are also known to process internalized epidermal growth factor receptors (EGFR) en route to the lysosome (Hopkins et al., 1990; Futter et al., 1996) and thus, there is good reason to expect that the endosome compartments of polarized cells will be found to contain a variety of sorting mechanisms. Recent studies on these compartments have shown them to be extensively interconnected and have identified the exocytotic vesicles that carry TR to the basolateral border (Odorizzi et al., 1996). In a recent paper (Futter et al., 1998) we have demonstrated that these basolateral vesicles arise from clathrin/AP 1-coated buds on endosomal tubules but no other sorting mechanism has yet been identified on the apical transcytotic pathway of MDCK cells. The purpose of the work reported here is to locate the mechanisms that bring about the apical transport of dIgA/pIgR complexes and relate them to the sorting mechanisms already known to operate in endosomal compartments.

Using electron microscopy to follow the apical transcytotic pathway taken by dIgA, the physiological ligand of pIgR, we show that dIgA/pIgR internalized from the basolateral surface at 20°C become distributed throughout groups of interconnected vacuoles and tubules which also contain internalized TR and EGFR. These groups of endosome elements sort the mixed pool of internalized receptors they contain by partitioning them into specialized domains on their perimeter membranes. The partitioning of pIgR is brought about by a novel, microtubule-dependent process which generates apically orientated tubules whilst TR are being selectively removed via 60-nm clathrin-coated buds and EGFR are being removed to the intraluminal vesicles of multivesicular bodies (MVB). In dIgA-induced tubules, the initial partitioning of dIgA/pIgR complexes is further refined by a process of maturation during which TR continue to be removed and which produces free, cup-shaped vesicles enriched in pIgR.

## Materials and Methods

### Reagents

dIgA was generously supplied by R. Drew (Birmingham University, Birmingham, UK) and dIgA tracers and all other reagents and radiolabels were prepared by the same procedures as described previously (Odorizzi et al., 1996). Colloidal gold sols were made as described (Slot and Geuze, 1985).

### Cell Culture and Incubation Conditions

Two kinds of MDCK cells were used and for studies on polarized monolayers, they were plated onto 24-mm Transwell filters (Costar Corp., Cambridge, MA) and used after 4–10 d in culture. PIR II cells were MDCK strain I cells transfected with a PLK-neo vector containing the cDNA for the wild-type rabbit pIgR (Hirt et al., 1993). Receptor expression was induced by treating with 1  $\mu$ M dexamethasone (Sigma Chemical Co., St. Louis, MO) in serum-free DME for 16 h. In control unstimulated cells the uptake of dIgA-HRP tracer was undetectable.

MDCK cells expressing pIgR and TR were generated by infecting

MDCK strain II cells expressing the receptor for Rous sarcoma virus(A) (Bates et al., 1993) and expressing human TR with BH-RCAS(A)-pIgR. The recombinant retrovirus vector was made from a plasmid containing the cDNA for rabbit pIgR (provided by K. Mostov, University of California, San Francisco, CA) digested with BglIII to excise the 2.4-kb insert. ClaI linkers were added to this fragment which was then ligated into the ClaI site of the replication competent vector BH-RCAS(A) (Odorizzi and Trowbridge, 1994).

Cells were maintained, grown as polarized monolayers, and receptor expression was increased by sodium butyrate treatment and incubated with tracers as described (Odorizzi et al., 1996). Measurement of radiolabeled ligand traffic and degradation were performed as described previously (Futter et al., 1996).

### DAB Cross-linking for Quantitative Studies

Cells on filters incubated with HRP-conjugated and iodinated ligands and with surface-associated ligand removed were washed at 4°C with TBS incubated in TBS containing 300  $\mu$ g/ml DAB and 0.015% H<sub>2</sub>O<sub>2</sub> at 4°C for 30 min. Filters were excised and incubated two times for 15 min each at 48°C in TBS containing 1% Triton X-100 (TX100) and 0.02% azide. The TX100 washes and the filter were counted in a gamma counter. The percent cross-linking was determined by comparing TX100 washes and filter-associated radioactivity.

### Light Microscopy

Cells growing on coverslips were rinsed free of serum and incubated with fluorescent tracer as appropriate. They were then rinsed free of unbound tracer and surface dIgA was removed by incubation with proteinase K (25  $\mu$ g/ml) for 15 min at 5°C. Cells were processed for light microscopy as described previously (Odorizzi et al., 1996).

For video microscopy, images were collected with a Hamamatsu C4880 dual mode cooled charge-coupled device (CCD) camera from a 63 $\times$  NA 1.4 planapochromat objective on a Zeiss 135M Axiovert microscope (Carl Zeiss Inc., Thornwood, NY) maintained in a 37°C incubator. Images were acquired onto the CCD chip at a magnification of 100 nm/pixel. For excitation, a halogen lamp set at 3–5 V replaced the mercury vapor lamp. Exposure time of 1 s was controlled by a Uniblitz D-122 shutter at 20- or 30-s intervals. Individual frames were converted to Windows AVI movie format at 15 frames/s giving a 300–450 $\times$  playback rate.

### Electron Microscopy of Polarized Monolayers

Monolayers were stimulated overnight with either dexamethasone or butyrate, rinsed free of serum and then incubated with tracers. For most experiments monolayers were incubated at 20°C for 60 min with tracer in the basolateral medium. They were then incubated at 37°C, with or without dIgA as appropriate, before being fixed, treated with DAB/H<sub>2</sub>O<sub>2</sub>, embedded, and sectioned as described previously (Odorizzi et al., 1996). Sections were analyzed morphometrically using standard techniques as described in Weibel (1979).

### Localization of Receptors by Electron Microscopy

Cells were loaded with HRP tracers (dIgA-HRP or Tf-HRP) and/or gold conjugates (dIgA-gold, B3/25-gold) at 20°C for 60 min. They were then rinsed in ascorbic acid buffer (20 mM Hepes, 70 mM NaCl, 50 mM ascorbic acid, pH 7.0) at 5°C to inhibit HRP activity on the cell surface (Stoorvogel et al., 1996), incubated for 0–60 min at 37°C in ascorbic acid with 0.2  $\mu$ g/ml dIgA as appropriate. Intracellular compartments containing HRP activity were cross-linked by incubation with 750  $\mu$ g/ml DAB and 0.015% H<sub>2</sub>O<sub>2</sub> in ascorbic acid buffer. The cells were then permeabilized by incubating in 40  $\mu$ g/ml digitonin in permeabilization buffer (25 mM Hepes, 38 mM aspartate, 38 mM glutamate, 38 mM gluconate, 2.5 mM MgCl<sub>2</sub>, 2 mM EGTA, pH 7.2). They were then fixed in 2% paraformaldehyde, quenched with 15 mM glycine and blocked with 1% BSA before being incubated with gold antibody conjugates (anti-tail pIgR [166]) (Hirt et al., 1993) and/or anti-tail TR (H68.4) (White et al., 1992). Finally, they were fixed in 2.5% glutaraldehyde, embedded in Epon and prepared for thin-section electron microscopy.

### Quantitation of pIgR and TR Gold Labeling

pIgR and TR were quantitated in double-labeled, digitonin-permeabilized preparations using 166 and H68.4 antibody-gold conjugates. The number

of 5 (TR) and 10 nm (pIgR) gold particles on vesicles containing internalized dIgA-HRP/Tf-HRP were counted after 40 min at 37°C. The vesicles were divided into those above 100 nm in diameter (the majority of which are cup-shaped at this time) and 60-nm-diam “basolateral” vesicles (which have a distinctive shape and content) (Futter et al., 1998). The experiment was carried out twice and in each experiment up to 372 vesicles were counted. Counts were made on batches of 30 randomly selected vesicles and there was less than 3% variation between batches. It is important to note that the sensitivity of labeling varies with gold size. Thus, when TR on 60-nm-diam vesicles are labeled with 10- rather than 5-nm-diam gold complexes, the number of particles bound per vesicle is significantly reduced and cannot be used for comparative labeling. Indeed, when vesicles as small as 60 nm are labeled simultaneously with 5-nm anti-TR and 10-nm anti-pIgR there is a detectable reduction in the level of TR label. Thus, although the Stokes’s radius of 5-nm gold complexes is likely to be similar to that of individual receptors, steric hindrance probably causes some interference with labeling when the vesicle diameter is as small as 60 nm. For comparative quantitative analysis of pIgR and TR and to obtain optimum sensitivity for TR, 100- and 60-nm vesicles were therefore labeled simultaneously with 5-nm anti-TR and 10-nm anti-pIgR.

### **Whole Mount Preparations for Electron Microscopy**

For whole mounts, cells growing on coverslips were treated as above but instead of being permeabilized with digitonin, they were extracted with 1% TX100 in PBS containing 1mM MgCl<sub>2</sub>, 0.1 mM CaCl<sub>2</sub>, and 0.02% azide for 10 min at 5°C. After being labeled with gold conjugates, cells were fixed in 4% glutaraldehyde and dehydrated before being prepared for carbon replicas as previously described in detail (Hopkins, 1985).

## **Results**

### **The Transcytotic Pathway Followed by dIgA Tracers in Polarized MDCK Cells at 37°C**

Using dIgA-HRP and dIgA-gold tracers, the basal to apical transcytotic pathway was outlined in MDCK monolayers expressing pIgR from a dexamethasone inducible vector (PIR II cells). After incubations at 37°C for periods of up to 60 min the tracers were present in coated pits on the basolateral plasma membrane, within a variety of 0.1–0.3- $\mu$ m-diam vacuoles and in 60- and 100-nm-diam tubulovesicles distributed throughout the apical cytoplasm (Fig. 1). Initially the majority of the vacuoles lack internal vesicles and are surrounded by tubules and vesicles but, after incubations of 10 min or more, vacuoles recognizable as typical MVB and loaded with dIgA tracer develop (Fig. 1 b). 0.5- $\mu$ m-thick sections were used to determine if profiles containing dIgA-HRP belonged to tubules or free vesicles. They showed long (> 3.0  $\mu$ m), 100-nm-diam tubules lying parallel to microtubules (Fig. 1 e) and orientated towards the apical cytoplasm and distinctive, 100–150-nm-diam cup-shaped vesicles distributed immediately below the apical plasma membrane. Centrioles, which also lie below the apical membrane in these cells, are usually surrounded by clusters of tubules and free, cup-shaped vesicles (Fig. 1 b). In MDCK cells expressing pIgR and TR, all of the structures that load with dIgA-HRP in PIR II cells are identifiable and DAB-positive.

### **Cup-shaped Vesicles Are Apical Transcytotic Vesicles**

The apical surface of cells loaded basolaterally with dIgA-HRP becomes coated with fine, DAB-positive filaments (Fig. 1 c). These filaments can be removed with proteinase K (25  $\mu$ g/ml) and if a competitive peroxidase substrate (50 mM ascorbic acid) is included in the apical medium, DAB reaction product can be prevented from forming on the

apical membrane. We believe these DAB-positive filaments to be dIgA-HRP/pIgR which have transcytosed to this surface but remained uncleaved. Undispersed cores of DAB-positive material can also be found in exocytotic invaginations on the apical surface (Fig. 1 d) clearly indicating that these complexes are delivered to this surface by exocytosis. If protease and ascorbic acid are included in the apical medium during 37°C incubations with dIgA-HRP in the basal medium large numbers of cup-shaped vesicles containing dIgA tracer continue to be produced. This suggests that most, if not all, dIgA-HRP in cup-shaped vesicles is derived from an intracellular source, that is, directly from the transcytotic pathway.

### **Tubules and Cup-shaped Vesicles Are Produced upon Transfer to 37°C**

Morphometric analysis of electron micrographs (Fig. 2) shows that in cells loaded with dIgA-HRP at 20°C for 60 min most of the tracer is distributed in small, pleomorphic endosomal elements whose total surface area comprises 73.75% of the membrane surrounding HRP-positive endosomal structures. The remainder of the membrane surface on elements containing dIgA-HRP is distributed between 0.1–0.3- $\mu$ m vacuoles (12.29%), 50–100-nm-diam tubules (3%), and 100-nm-diam cup-shaped vesicles (10.96%). Upon shifting to 37°C the relative proportions of these elements change (Fig. 2) so that after 15 min there is a dramatic increase in the number of tubules. During an additional 15 min however, the number of tubules declines whilst the number of cup-shaped vesicles increases. In the second 15 min, the increase in cup-shaped vesicles is twice as large as in the first 15 min. During the 30 min at 37°C the proportion of endosome membrane surrounding 0.1–0.3- $\mu$ m-diam vacuoles falls from 12.29 to 1.21%. These data show that upon transfer to 37°C, internalized dIgA/pIgR cause major changes in the shape of the endosome compartment within filter-grown polarized cells. The changes observed suggest that upon shifting to 37°C, tubules form at the expense of vacuoles and indicate that the process of dIgA-induced tubulation observed in flat cells by video microscopy and described below also occurs in polarized filter-grown cells. The time of appearance of cup-shaped vesicles is also in keeping with the observations described below which show that these vesicles arise from tubules in flat cells. However, because the tubule/vesicle transformation process is difficult to demonstrate in filter grown cells, it has not been possible to make a quantitative analysis that directly demonstrates a precursor-product relationship at this step.

### **At 20°C pIgR, TR and EGFR Tracers Codistribute throughout the Endosome Compartment**

To follow differential sorting to apical and basolateral surfaces, polarized monolayers were first loaded with tracers at 20°C. The extent to which the receptors were contained in the same endosome elements was assessed under these conditions by cointernalizing HRP tracers with <sup>125</sup>I-labeled ligands then cross-linking them by incubation with DAB and H<sub>2</sub>O<sub>2</sub>. The efficiency of the cross-linking varies with the HRP conjugate but optimally levels up to 80% can be obtained with this technique (Courtoy et al., 1984). As

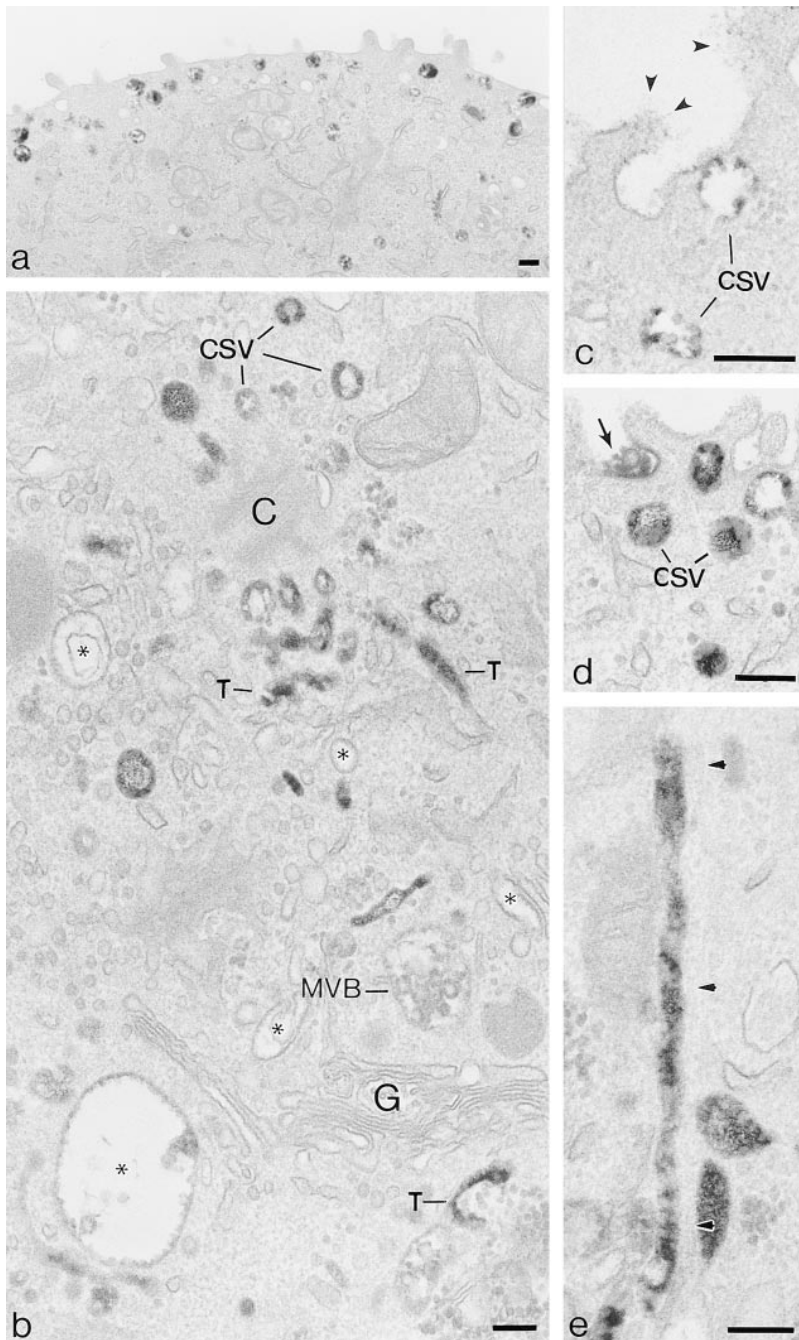


**Figure 1.** Transcytotic pathway of polarized PIR II MDCK cells outlined by dIgA-HRP internalized from the basolateral surface, 37°C. (a) Thick section showing dIgA-HRP loaded 100-nm-diam vesicles distributed below apical membrane. (The cup shape of these vesicles is more clearly shown at higher magnification in b). (b) Apical cytoplasm surrounding a centriole (C) and above Golgi stack (G). dIgA-HRP is distributed on the inner perimeter membranes of vacuoles (\*), within MVB (MVB), throughout 100-nm-diam tubules (T) and in 100-nm-diam cup-shaped vesicles (csv). (c) High magnification showing apical vesicles containing transcytosed dIgA-HRP; arrowheads, fine filaments of DAB reaction product distributed on the apical surface; csv, cup-shaped vesicles. (d) As c, an undispersed core of reaction product (arrow) identifies a site of exocytosis. (e) 100-nm-diam tubule containing dIgA-HRP running in the long axis of the cell; arrowheads, position of microtubule. Bars, 0.2  $\mu$ m.

shown in Table I, basolaterally applied dIgA-HRP and fluid-phase HRP cross-link between 62 and 72% of basolaterally applied  $^{125}$ I-IgA and  $^{125}$ I-EGF.

In agreement with the observations made in our previous studies (Odorizzi et al., 1996; Futter et al., 1998) electron microscopy confirmed these cross-linking data by showing that pIgR and EGFR tracers become codistributed throughout most of the endosomal vacuoles that can be loaded with TR tracers at 20°C (data not shown but see below).

#### **Transfer to 37°C Induces Differential Processing of dIgA, Tf, and EGF**

When filter-grown monolayers of MDCK cells are pre-

loaded basolaterally with tracer for 60 min at 20°C and then shifted to 37°C, the internalized tracers are selectively sorted. The kinetics of dIgA and Tf release at 37°C from cells expressing pIgR and TR and preloaded at 20°C have been described previously (Futter et al., 1998) and for the present study it is necessary to note only that after 60 min at 37°C,  $71.7 \pm 0.9\%$   $^{125}$ I-Tf is released basolaterally and  $21.3 \pm 0.9\%$  is released apically. The figures for  $^{125}$ I-dIgA are  $50.7 \pm 1.0\%$  apical and  $20.4 \pm 0.7\%$  basolateral. The kinetics of release of  $^{125}$ I-dIgA from PIR 11 cells is significantly slower (Fig. 3) but at 3 h, when it shows signs of approaching steady state, the apical/basolateral ratio of release 60:20% is similar. During this time 80% of the internalized  $^{125}$ I-EGF is retained within the cell and degraded. During the 4-h incubation at 37°C, less than 10%

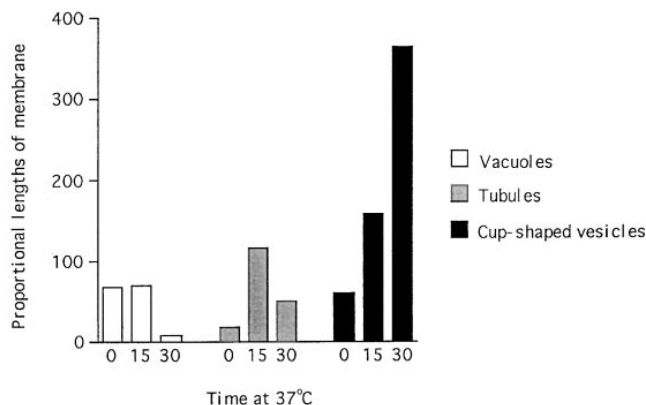


**Figure 2.** Changes in proportions of dIgA-HRP containing vacuoles, tubules, and cup-shaped vesicles in polarized, filter-grown cells on transfer to 37°C. Polarized, filter-grown cells were loaded with dIgA-HRP at 20°C and then transferred to 37°C for 0, 15, and 30 min. With time at 37°C the proportion of vacuoles decreases, the proportion of tubules increases and then decreases, and the proportion of cup-shaped vesicles increases. The increase in cup-shaped vesicles is twice as rapid in the second 15-min interval. The data were obtained by estimating the surface area of all dIgA-HRP-containing elements within equivalent areas of cytoplasm in cells incubated for the 0–30-min time intervals and then assigning them to four groups; elements of less than 60-nm-diam, vesicles of 100-nm-diam (i.e., cup-shaped vesicles), tubules of 100-nm-diam, and elements of 0.1–0.3- $\mu$ m-diam (vacuoles). Elements of less than 60 nm in diameter comprised 74% of the total DAB-positive structures.

of the preloaded  $^{125}$ I-dIgA is degraded. In similar circumstances Tf degradation was also found to be negligible (Odorizzi et al., 1996).

### Morphological Characterization of the Sorting Process

To study the formation of cup-shaped, transcytotic vesicles in more detail, cells were grown to subconfluence on solid substrata (usually glass coverslips) and incubated overnight in 10 mM butyrate. Under these conditions the cells spread to become extremely flat. This morphology allows the form and movement of endosomes loaded with fluorescent tracers to be analyzed in detail by video microscopy and whole mounts (Hopkins, 1985) can be prepared for correlative electron microscopy.

### dIgA Induces Tubulation of Endosomal Vacuoles

In preparations loaded to steady state at 20°C with dIgA-

**Table I.** Percent Cross-linking of  $^{125}$ I Tracers by HRP Conjugates

|                      | MDCK (PIR II) Monolayers<br>(expressing plgR) |                     |
|----------------------|---|---------------------|
|                      | $^{125}$ I dIgA baso                          | $^{125}$ I EGF baso |
| Fluid-phase HRP baso | 69.6 $\pm$ 4.0                                | 72.2 $\pm$ 3.1      |
| dIgA-HRP baso        | —   | 62.5 $\pm$ 1.7      |

Cells on filters incubated with HRP-conjugated and radiolabeled ligands in the basolateral medium as indicated.

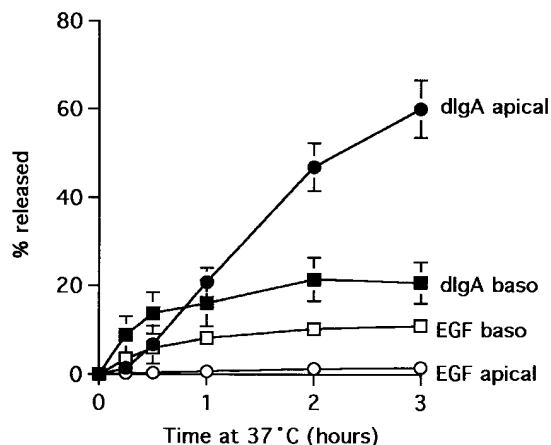


**Figure 3.** Release of dIgA and degradation of EGF in polarized PIR II cells. Monolayers were preloaded basolaterally at 20°C with  $^{125}$ I-dIgA (solid symbols) or  $^{125}$ I-EGF (open symbols), chased at 37°C and apical (circles) and basolateral (squares) media collected. For EGF, only TCA-precipitable protein released is shown.

FITC, up to 150 individual vacuolar structures can be identified in each cell (Fig. 4 a). Video microscopy of living cells shows that these vacuoles often stay grouped together in closely packed clusters for periods of 15 min and longer (see Fig. 5) and during this time there are continuous changes of shape, form, and position (see video recording on <http://www.ucl.ac.uk/lmcb/gibson.htm>). As described below, electron microscopy shows that many of the vacuoles in these clusters are interconnected by narrow tubules that are difficult to resolve by fluorescence microscopy.

When cells preloaded with dIgA-FITC are transferred from 20° to 37°C, long tubules loaded with tracer grow from the clusters of endosome vacuoles (Fig. 4 b and Fig. 5 b). These tubules also develop in cells loaded at 20°C with Tf-FITC (Fig. 4 e), but only if they are transferred to 37°C in the presence of dIgA (Fig. 4 f). Double labeling shows that the tubules containing dIgA-FITC are the same as those induced in cells preloaded with Tf-Texas red (data not shown). The tubules are transient, becoming maximally developed after 15 min at 37°C and disappearing by 30 min. Tubule breakdown occurs rapidly, first into elongated fragments and then into fine punctate dots that distribute throughout the cytoplasm. In some cells this fine punctate fluorescence is seen to be concentrated around centrioles (Fig. 4 c).

### dIgA-induced Tubulation Requires Intact Microtubules

The tubulation process can be observed in cells preloaded with either dIgA-FITC or Tf-FITC but does not occur in the absence of dIgA (Fig. 4 f). If cells are preloaded at 20°C, incubated at 5°C for 60 min with 15  $\mu$ m nocodazole, and then incubated at 37°C with dIgA tubules do not form. Cells loaded with dIgA-FITC at 20°C and treated with nocodazole vacuoles retain their fluorescence with subsequent incubation at 37°C (Fig. 4 d).

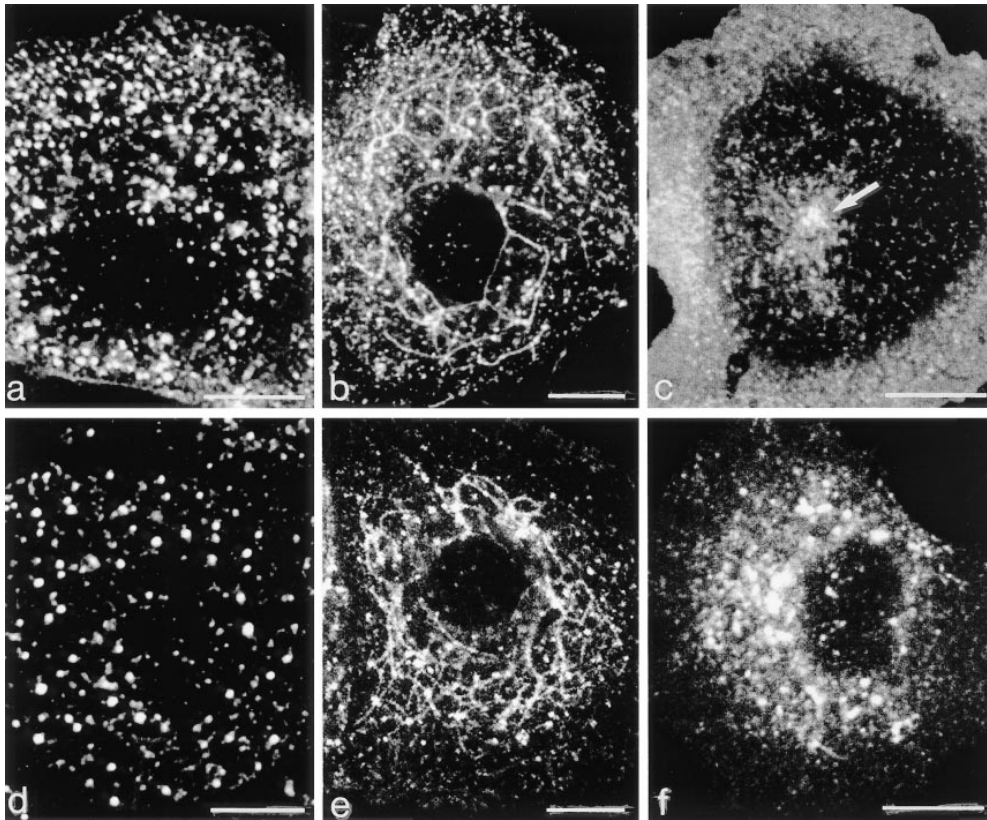


**Figure 4.** The distribution of fluorescent dIgA and Tf in pIgR/TR-expressing cells grown on glass coverslips. (a) Cells loaded with dIgA-FITC at 20°C for 30 min. Brightly fluorescing vacuoles of sorting endosome complexes are distributed throughout the cytoplasm. (b) As in a, then transferred to 37°C for 10 min. Long, dIgA-FITC-containing tubules have formed. (c) As in a, then transferred to 37°C for 30 min. Tubules replaced by fine punctate fluorescence distributed throughout peripheral cytoplasm. *Arrow*, pericentriolar concentration of dIgA fluorescence lying below the nucleus. (d) Cells preincubated with nocodazole 30 min at 5°C then treated as in c. Tubules do not form and the number of sorting endosome vacuoles is only slightly reduced compared with the 20°C condition shown in a. The vacuoles remain brightly fluorescent for dIgA and should be compared with the structures

shown by electron microscopy in Fig. 6 d. (e) Cells loaded with Tf-HRP at 20°C for 30 min and then transferred to 37°C for 10 min in the presence of dIgA. Tubules are displayed. (f) Cells treated as in e but no dIgA added on transfer to 37°C. No tubules form. Bars, 10 μm.

### Analysis of Receptor Distributions by Electron Microscopy

To follow the intracellular processing of the internalized tracers by electron microscopy, flat cells were loaded at 20°C with HRP tracers (fluid-phase HRP, Tf-HRP, or dIgA-HRP). In some experiments, gold-labeled dIgA or anti-EGFR gold complexes were included with the HRP tracers. The cells were incubated with ascorbic acid to block surface HRP activity (refer to Materials and Methods) and then with DAB/H<sub>2</sub>O<sub>2</sub> at 5°C, a treatment that has been shown by Stoorvogel et al. (1996), to cross-link the contents of compartments containing the internalized peroxidase. The cells were then permeabilized with digitonin, fixed, and then the cytoplasmic domains of the receptors on the surfaces of the cross-linked endosomal elements were labeled with immunogold procedures. This approach allows distributions of both occupied and unoccupied receptors to be mapped and for specimens to be used either for embedding and sectioning or for whole mounts.

Sections of embedded preparations from flat cells grown on solid substrates show that pIgR, TR, and EGFR tracers internalized at 20°C codistribute throughout the vacuolar and tubular elements of the endosome compartment (Fig. 6). To quantitate the tubulation process, cells were loaded with Tf-HRP at 20°C and then transferred to 37°C in the presence of dIgA. As shown in Table II, morphometric analysis of structures containing DAB indicates that the dIgA treatment increases the proportion of tubules from 33.0 to 55.4%. These preparations also show that when these

cells are transferred to 37°C they package dIgA-HRP into vesicles with a morphology identical to the 100-nm-diam cup-shaped vesicles seen at the apical borders of filter-grown polarized cells (see Fig. 9 d).

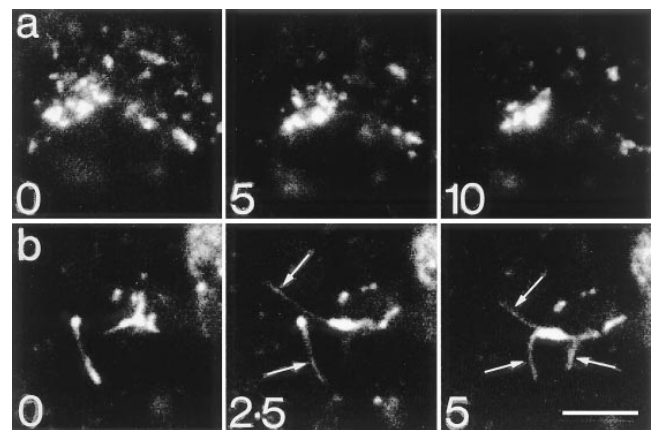


**Figure 5.** Video microscopy of endosomes at 20° and 37°C. (a) Stills taken from video in which cells grown flat were incubated with dIgA-FITC at 20°C for 60 min. Over the 10-min period the cluster of brightly fluorescent vacuoles continually changes shape and position but remains grouped together. (b) As in a but cells transferred to 37°C. During this 5-min interval, fine tubules (*arrows*) grow rapidly from the vacuole. (The full sequences of these videos can be seen on <http://www.ucl.ac.uk/lmcb/gibson.htm>). Bars, 5 μm.

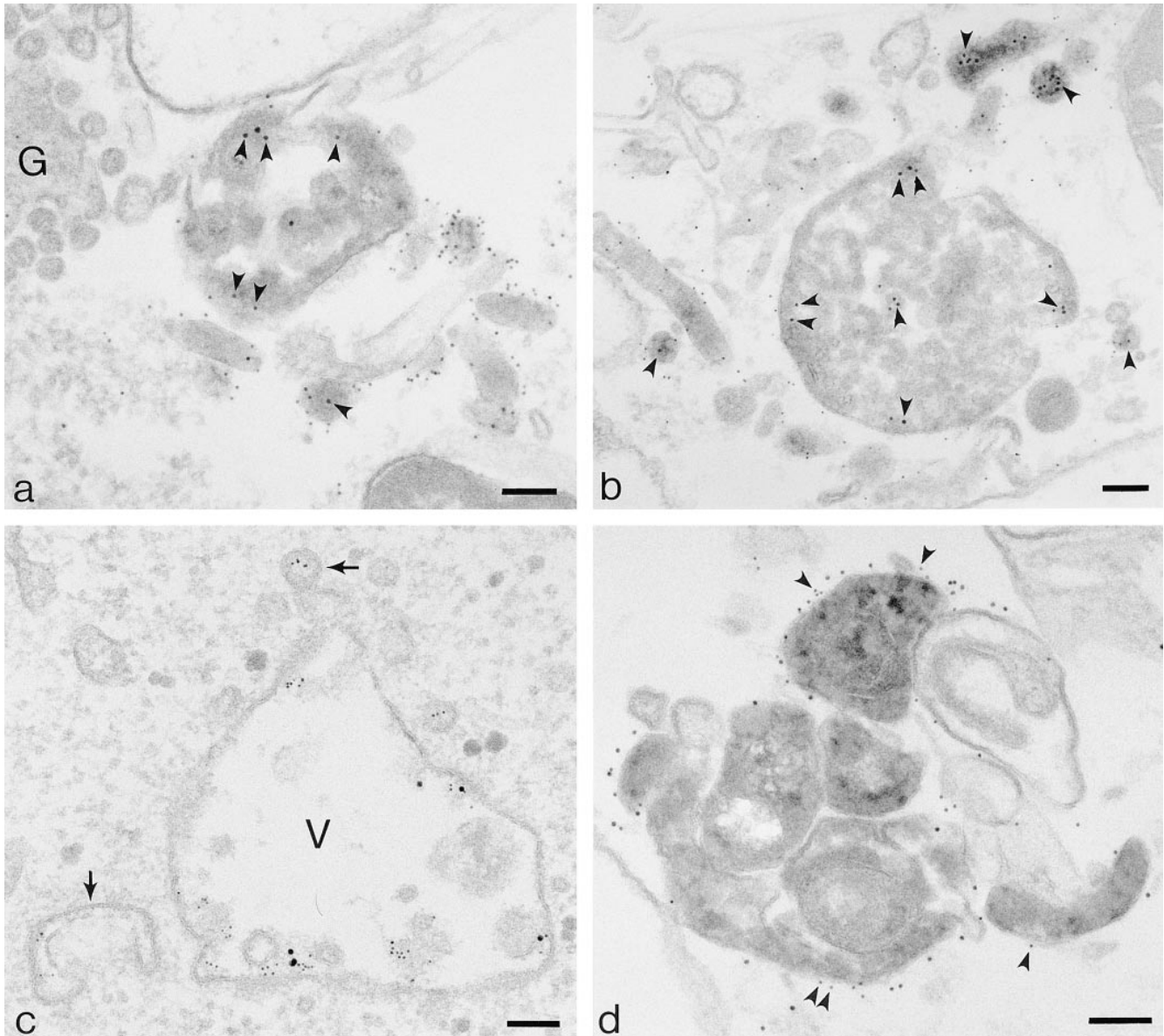


**Figure 6.** Colocalization of pIgR, TR, and EGFR tracers in clusters of endosome vacuoles and tubules in cells growing on solid substrata. (a) Vacuoles and tubules containing internalized dIgA-HRP and 10-nm gold/anti-TR (*arrowheads*). The cytoplasmic domains of pIgR are labeled with 5-nm gold and show them to be distributed throughout the dIgA-HRP-loaded vacuoles and tubules. Vesicles surrounding the Golgi (G) are unlabeled. Cells were preloaded with dIgA-HRP and 10-nm gold/anti-TR at 20°C for 60 min. Internalized HRP cross-linked with DAB/H<sub>2</sub>O<sub>2</sub>, and cells permeabilized with digitonin before being labeled with 5-nm gold/anti-pIgR. (b) Vacuoles and tubules containing internalized Tf-HRP and 10-nm gold/dIgA. The cytoplasmic domains of TR are labeled with 5-nm gold. HRP-loaded vacuoles and most tubules that label with 5-nm gold/anti-TR also contain internalized pIgR tracer (*arrowheads*). Cells were prepared as in a. (c) Cells loaded with 10-nm gold/dIgA and 5-nm gold/anti-EGFR in presence of 200 ng/ml EGF at 20°C for 30 min. Sorting endosome vacuole (V) and associated tubules (*arrows*) contain both tracers. (d) Without microtubules, tubulation does not occur at 37°C and vacuoles remain loaded with dIgA-HRP/pIgR. These compact groups of vacuoles correspond to the strongly fluorescent spots seen in Fig 4 d. Cells were loaded with dIgA-HRP for 60 min at 20°C, incubated with nocodazole at 5°C for 30 min, and then incubated at 37°C for 40 min. Internalized dIgA-HRP cross-linked with DAB/H<sub>2</sub>O<sub>2</sub>, and cells permeabilized with digitonin before being labeled with 10-nm gold/anti-pIgR and 5-nm gold/anti-TR (*arrowheads*). Bars, 0.1 μm.

### ***pIgR and TR Are Distributed throughout IgA-induced Tubules***

Whole mounts of flat cells demonstrate that the clusters of endosome vacuoles observed by video microscopy are elaborately interconnected by narrow tubules (Fig. 7 a). Short tubules also extend from some of the more periph-

eral vacuoles. Gold labeling the cytoplasmic domains of TR and pIgR confirms that these receptors are distributed in a random fashion throughout the vacuoles and tubules of these interconnected complexes. The only indication of order in the distribution of the internalized receptors is shown in the tubules where internalized gold particles

**Table II. Percent Proportion of Structures Containing Internalized Tf-HRP**

| Time at 37°C | 0.1–0.3- $\mu$ m-diam vacuoles | 100-nm-diam tubules | 100-nm-diam cup-shaped vesicles | 60-nm-diam vesicles | Others: >60-nm diam |
|--------------|--------------------------------|---------------------|---------------------------------|---------------------|---------------------|
| 0 min        | 30.6                           | 33.0                | 1.9                             | 10.7                | 23.8                |
| 15 min       | 22.4                           | 55.4                | 2.4                             | 5.5                 | 14.2                |

Morphometric quantitation of DAB reaction product in cells grown on coverslips loaded with Tf-HRP at 20°C for 60 min and then incubated with dIgA at 37°C for 15 min. dIgA causes the proportion of DAB-positive structures identifiable as tubules to increase from 33 to 55%. The Tf-HRP tracer is not incorporated into cup-shaped vesicles as efficiently as dIgA tracers.

sometimes line up in single file. However, this is only seen with the larger (10-nm) internalized gold and is displayed by both pIgR and TR tracers. It is thus probably an artefact induced by internalized gold complexes.

When whole mounts are prepared from cells loaded at 20°C and shifted to 37°C in the presence of dIgA, the long

tubules seen to form by video microscopy are clearly displayed (Fig. 7 *b*). The tubules have diameters in the range of 130–150 nm and extend throughout the cell. They are found in addition to the narrower tubules seen in cells loaded with Tf-HRP but continuities between the narrower and wider form of the tubule are often seen (Fig. 8 *c*) and both can be found connected directly to 0.1–0.3- $\mu$ m-diam vacuoles.

Labeling the cytoplasmic domains of pIgR and TR on the tubulated endosomes of whole mounts shows that these receptor populations are randomly intermixed and evenly distributed along the length of the tubules (Fig 8, *inset*). In cells pretreated with nocodazole, IgA-induced tubules are not formed with subsequent incubation at 37°C. This result conforms with previous published studies (Hunziker et al., 1990) which showed nocodazole is a potent inhibitor of apical transcytosis in MDCK cells. If cells are preloaded at 20°C with dIgA-HRP, treated with nocodazole, and then incubated for 40 min at 37°C electron microscopy shows that most of the dIgA-HRP-positive

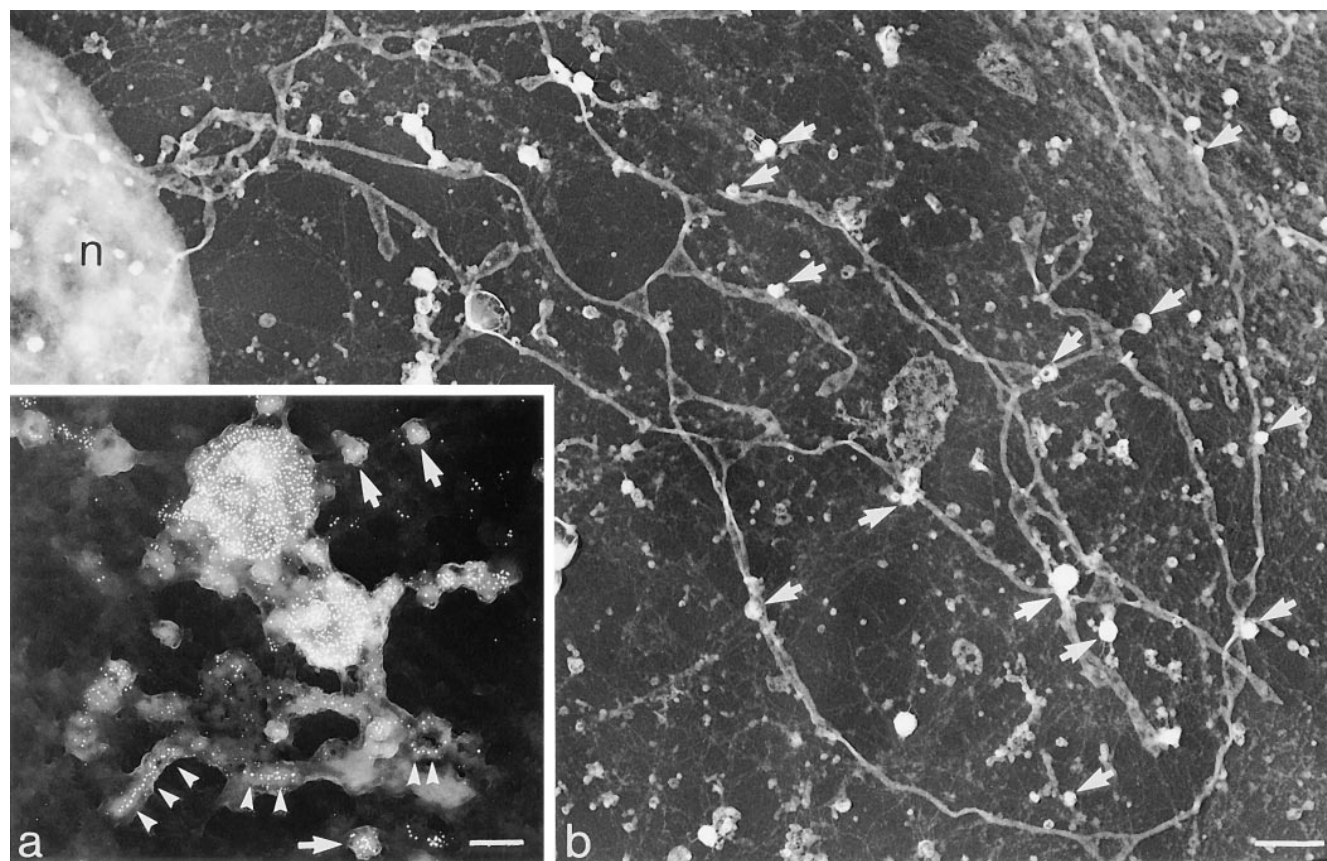


**Figure 7.** (a) Whole mount showing distribution of TR and pIgR in a complex of endosome vacuoles and tubules loaded with Tf-HRP at 20°C. (This complex corresponds to the structures seen in section in Fig. 6, *a–c*). The interconnected vacuolar and tubular elements of a sorting endosome complex have been preserved by cross-linking their content of Tf-HRP and dIgA-HRP. Internalized 10-nm-diam gold complexes show linearly arrayed pIgR within short tubules (*arrowheads*) and 5-nm gold particles identify the cytoplasmic domains of TR. *Arrows*, free vesicles. Both pIgR and TR are distributed throughout the complex. Cells preloaded with Tf-HRP, dIgA-HRP and 10-nm dIgA-gold at 20°C for 30 min, were cross-linked with DAB/H<sub>2</sub>O<sub>2</sub>, extracted with TX100, and then TR cytoplasmic domains were localized with TR antibody (H68.4) followed by 5-nm immunogold. Bar, 0.2  $\mu$ m. (b) Whole mount showing tubulation induced by dIgA. Low magnification view showing dIgA-induced tubules extending throughout the cytoplasm (Fig. 7 *a*) with vacuoles (*arrows*) distributed at intervals along their length. Cell preloaded with dIgA-HRP and Tf-HRP at 20°C for 30 min and transferred to 37°C for 15 min before being cross-linked with DAB/H<sub>2</sub>O<sub>2</sub>, extracted with TX100, and then labeled with antibody gold complexes (not evident in this micrograph, but see Fig. 8 *a*). *n*, nucleus. Bar, 1  $\mu$ m.



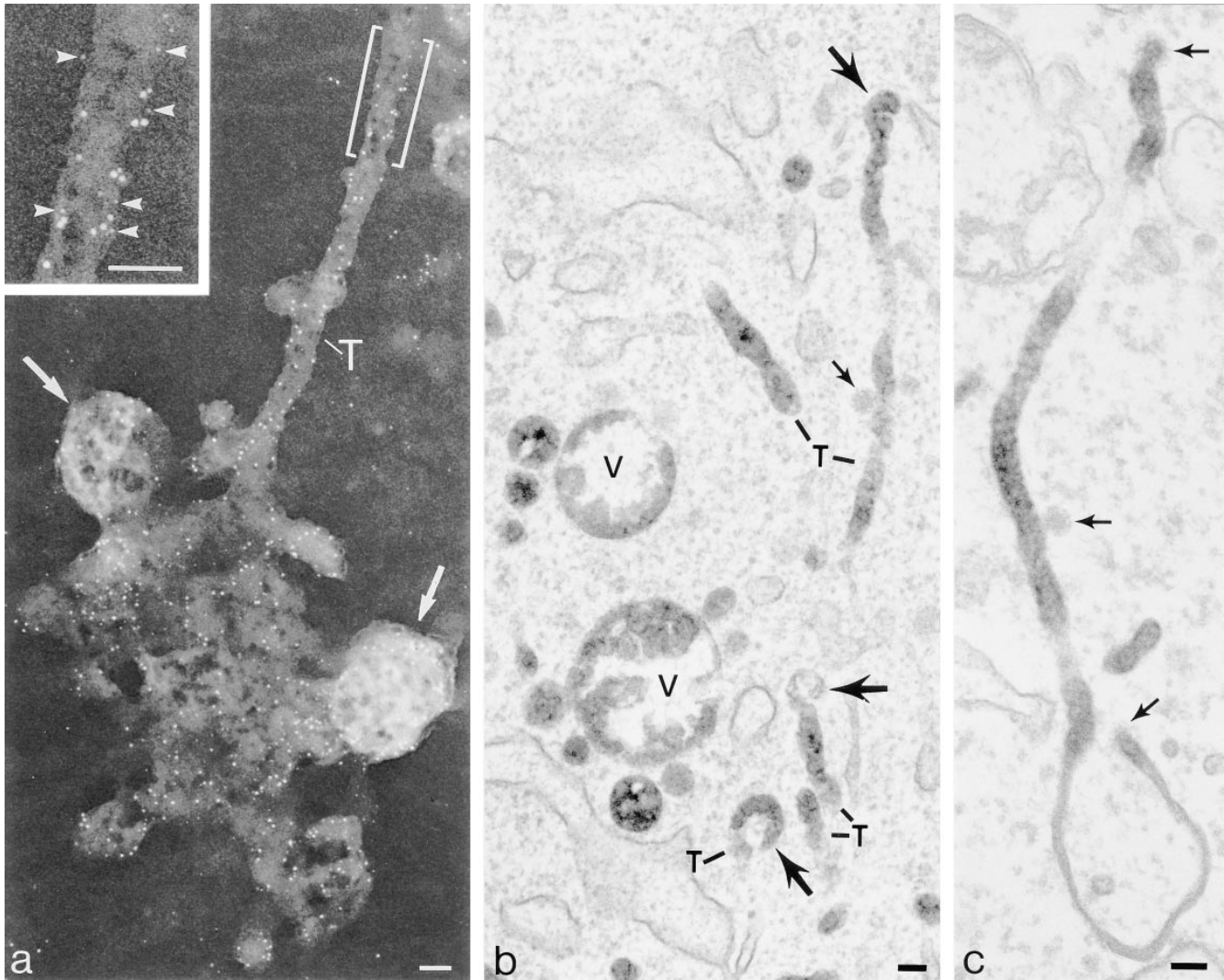


**Figure 8.** dIgA-induced tubules extending from clusters of endosome vacuoles. (a) Whole mount showing group of vacuoles including MVBs (arrows) with 100-nm-diam tubule extension (T). Gold particles show pIgR (10 nm) and TR (5 nm) distributed randomly throughout vacuoles and tubule. *Inset*, segment of tubule enlarged to display TR (arrowheads) distributed amongst pIgR. Cells were preloaded with dIgA-HRP and Tf-HRP at 20°C for 30 min and transferred to 37°C for 10 min before being cross-linked with DAB/H<sub>2</sub>O<sub>2</sub>, extracted with TX100, and then labeled with antibody gold complexes. (b) A group of vacuoles (V) and tubular extensions (T) similar to the interconnected complex shown in a but displayed in a conventional thin section. *Large arrow*, bulbous tips of tubules with invaginations similar to those seen in cup-shaped vesicles; *small arrows*, 60-nm-diam-coated vesicle. Cells preloaded at 20°C with dIgA-HRP and then transferred to 37°C for 10 min. (c) IgA-induced tubule varying in diameter from 50 to 120 nm. *Arrows*, coated buds. Cells were preloaded at 20°C with dIgA-HRP and then transferred to 37°C for 10 min. Bars, 0.1 μm.

vacuoles that remain contain pIgR (refer to Fig. 6 d). However, levels of TR and EGFR are low or undetectable in these vacuoles suggesting that these receptors can be recycled and transferred to the lysosome in the absence of polymerized microtubules.

#### **The Transformation of IgA-induced Tubules into Cup-shaped Vesicles**

Most dIgA-induced endosomal tubules bear clathrin lattices either on discrete buds distributed along their length or in more extensive domains at their ends (Figs. 8 and 9). When these coated structures are distributed on buds or on vesicles adjacent to the tubules they have diameters in

the range of 50–60 nm. In a related study on polarized cells (Futter et al., 1998) we have shown that buds on endosome tubules give rise to 60-nm-diam vesicles destined for the basolateral border. The buds on dIgA-induced tubules appear to be identical to those observed on tubules in cells loaded with Tf-HRP. It is possible to label adaptor proteins within these buds and show they contain AP 1 (Fig. 9 a) but these coated domains do not usually label with antibodies directed to the cytoplasmic tails of receptors. However, internalized gold tracers show that these coated buds contain both pIgR and TR (Fig. 9, b and c, and Futter et al., 1998). In unpublished studies we have also localized AP 3 adaptors (Simpson et al., 1996) in these cells and shown that most of the AP 3 labeling localizes to Lamp

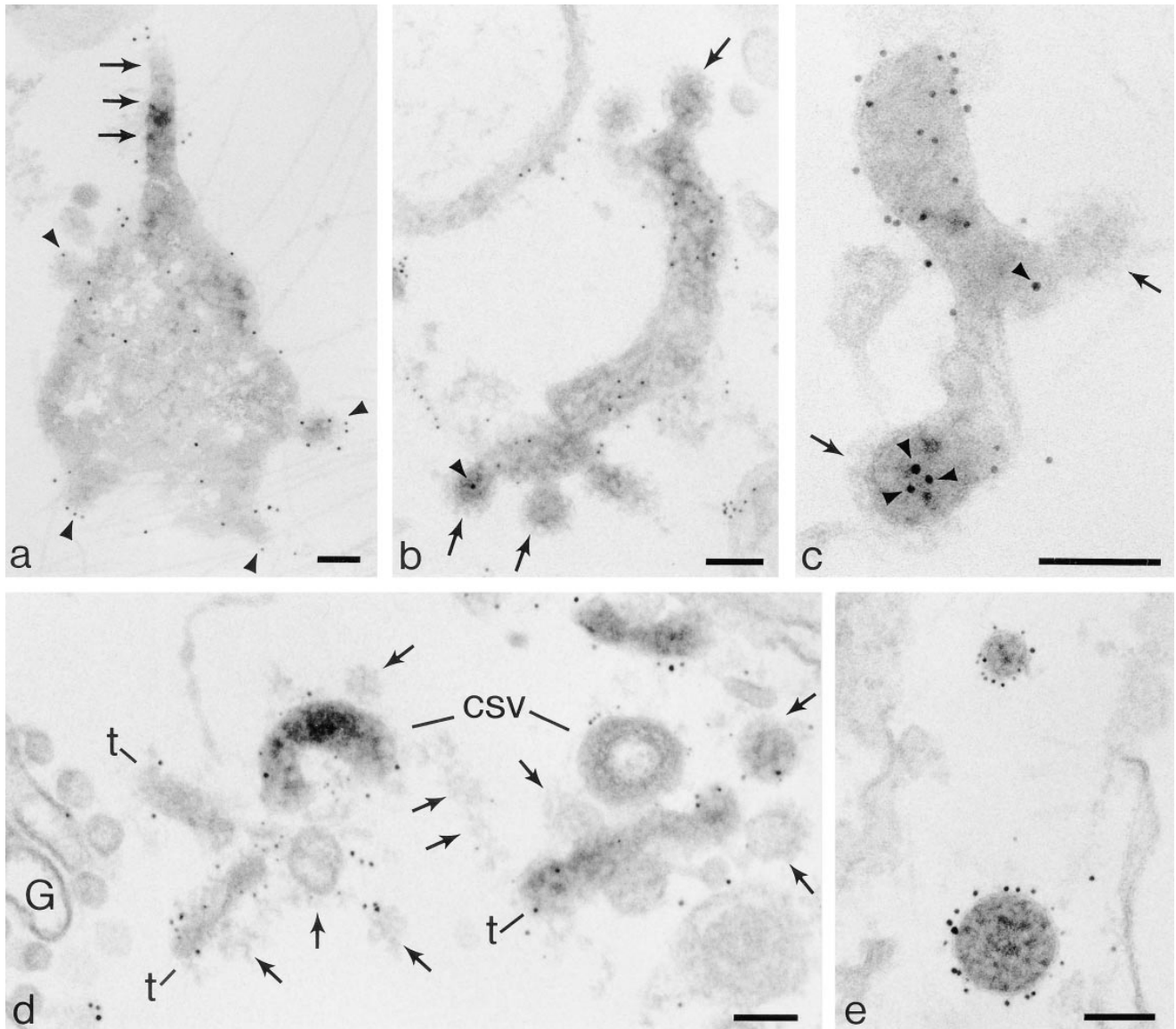


**Figure 9.** Distribution of pIgR and TR and their relationship to clathrin coats on vacuoles, fragmenting tubules, and on cup-shaped vesicles. (a) Distribution of AP 1 gold label on coated buds forming on an endosome vacuole (arrowheads) that is also giving rise to a 100-nm-diam dIgA-induced tubule (arrows). Immunogold labeling was as described in Futter et al., 1998. Cells were incubated with dIgA-HRP, Tf-HRP at 20°C for 60 min and then transferred to 37°C for 10 min. (b) Cytoplasmic domains of pIgR labeled with 5-nm gold on a fragment of a dIgA-induced tubule containing internalized 10-nm gold/anti-TR (arrowhead). Arrows indicate the distributions of clathrin lattices. Cells were incubated with dIgA-HRP, Tf-HRP at 20°C for 60 min, incubated with B3/25-gold at 5°C for 30 min, and then transferred to 37°C for 5 min. (c) Preparation as in b showing tubule fragment on which cytoplasmic domains of pIgR are labeled with 5-nm gold. Receptors within clathrin-coated domains (arrows) remain unlabeled but the presence of B3/25 gold (arrowheads) shows they contain TR. (d) Cup-shaped vesicles (csv) developing from tubule fragments, cytoplasmic domains of pIgR (10 nm), and TR (5 nm) labeled with gold. Arrows, clathrin lattices on tubule fragments (t); G, Golgi cisternae. Cells were preloaded at 20°C with dIgA-HRP and Tf-HRP and then transferred to 37°C for 15 min. The internalized HRP tracers have been cross-linked with DAB/H<sub>2</sub>O<sub>2</sub>. Cells were then permeabilized with digitonin and double labeled with gold antibody conjugates. (e) Distribution of pIgR (10-nm gold) and TR (5-nm gold) on 100-nm-diam vesicles (cup-shape not shown in this section) and 60-nm-diam vesicles. Membrane boundaries are visible, indicating that the section plane is close to equatorial in both vesicles. Both vesicles label for pIgR and TR but quantitation of these vesicle populations shows pIgR are more concentrated (60:40) in the larger vesicle and TR more concentrated (70:30) in the smaller. Bars, 0.1 μm.

1-positive vacuoles located in the later stages of the endocytotic pathway. We have not detected the AP 3 adaptor complexes on any structures containing internalized dIgA tracers.

In flat cells video studies show that the dIgA-induced tu-

bules that form on transfer to 37°C break up within a well defined interval of 10–15 min. Initially elongate fragments are produced and then the number of punctate dots, which electron microscopy shows represent 100- and 60-nm-diam vesicles, increases (refer to Fig. 4 c). Sections prepared

from cells fixed when tubules are forming show frequent dIgA-HRP-loaded profiles of tubules that terminate in cup-shaped vesicles. These profiles suggest that these vesicles can arise at this stage by budding from the bulbous tips of the tubules (Fig. 8 *b*). In cells fixed after 10–15 min at 37°C, that is, during the tubule fragmentation stage, clathrin-coated lattices are seen distributed over the surfaces of tubule fragments (Fig. 9 *a*) and cup-shaped vesicles are often identifiable among them (Fig. 9 *d*). Like the clathrin lattices on the dIgA-induced tubules, the lattices on these fragments contain AP 1 adaptors. We have not been able to detect any other form of coat structure on the fragmenting tubules or any aggregates of gold particles that would suggest that pIgR become selectively concentrated before they are packaged into cup-shaped vesicles.

### ***pIgR Are Enriched in 100-nm-diam Cup-shaped Vesicles, TR Are Enriched in 60-nm-diam Vesicles***

The number of pIgR and TR packaged into the exocytotic vesicles of flat cells was quantitated by double labeling with gold complexes carrying antibodies to the cytoplasmic domains of pIgR and TR cytoplasmic domains (refer to Materials and Methods). Quantitation of the gold antibody complexes on the surfaces of the 100-nm-diam cup-shaped vesicles in cells transferred to 37°C for 40 min shows that 59.3% are pIgR and 40.7% are TR. As described in Materials and Methods, 5-nm gold complexes were used to label TR in this analysis because they detect lower levels of antigen than 10-nm complexes. A direct comparison of the densities of gold label on vesicles arising from the endosome with densities on the rest of the endosome is difficult because endosome vacuole/tubule morphology is extremely pleomorphic during tubule formation and fragmentation. The inaccessibility of the cytoplasmic tails of receptors located beneath coated domains adds to this difficulty. It is, nevertheless, possible to compare the concentrations of pIgR and TR on the different populations of vesicles that arise from the endosome. The concentrations of labeled pIgR and TR on cup-shaped vesicles were, therefore, compared with their concentrations on 60-nm-diam vesicles which correspond to the basolateral vesicles we have previously identified in polarized cells (Odorizzi et al., 1996). Thus, whilst the proportions of the labeled receptors on cup-shaped vesicles are 59.3% pIgR to 40.7% TR, their proportions on 60-nm-diam vesicles are 30.2% pIgR to 69.8% TR.

The pIgR/TR ratios on cup-shaped vesicles (60:40) and 60-nm-diam vesicles (30:70) as quantitated by gold labeling do not correspond exactly to the proportions expected from our measurement of <sup>125</sup>I-dIgA/<sup>125</sup>I-Tf released from the apical (50:20) and basolateral (23:75) surfaces of polarized cells at this 40-min time point (shown in detail in Futter et al., 1998). This is to be expected in view of the practical difficulties of labeling vesicles as small as 60-nm-diam to saturation with 5- and 10-nm particulate probes (refer to Materials and Methods). Nevertheless, this morphological quantitation clearly demonstrates that pIgR and TR, which have been internalized to the endosome at 20°C are selectively packaged into the two vesicle populations on transfer to 37°C and, given that we have chosen a combination of labels that underestimates the level of pIgR label

in order to maximally detect TR on 60-nm-diam vesicles (discussed in Materials and Methods), it is able to show that pIgR become selectively concentrated in cup-shaped vesicles and TR become selectively concentrated in 60-nm-diam vesicles.

### ***Discussion***

Previous studies using cDNA expression systems have established that membrane proteins trafficking through the endosomes of polarized epithelial cells carry routing signals in their cytoplasmic domains (for review see Trowbridge et al., 1993). The signals selected by the mechanisms that deliver proteins to basolateral surfaces include the tyrosine and dileucine motifs recognized by the clathrin/AP 2 lattices on the cell surface but it is also clear that in order to be fully effective for basolateral targeting these signals also need to include residues in addition to the two- and four-residue motifs that suffice for rapid internalization (Odorizzi et al., 1997; Mellman, 1996). In the ~100-residue cytoplasmic domain of pIgR there are two tyrosine-based motifs that enhance internalization (Okamoto et al., 1992) and one of these motifs lies within a 14-residue, juxtamembrane segment that can operate as a fully functional basolateral signal (Casanova et al., 1990, 1991). This 14-residue signal includes a serine (ser664) that becomes phosphorylated when pIgR is internalized. Phosphorylation on ser664 greatly reduces the efficiency with which pIgR recycle back to the basolateral surface and has been shown to be required for the efficient transcytosis of the receptor from the endosome (Casanova et al., 1990). Mutated pIgR that cannot be phosphorylated on residue 664 (i.e., when ser664 is replaced by alanine; ala664) recycle to the basolateral surface and are not efficiently transcytosed (Casanova et al., 1990). However, when occupied by dIgA, pIgR-ala664 transcytose to the apical surface with the same efficiency as the wild-type receptor (Hirt et al., 1993). These data suggest that the main influence exerted by phosphorylation on ser664 is to prevent internalized pIgR from recycling.

Phosphorylation of pIgR on ser664 both inhibits pIgR recycling and increases its apical transcytosis (Casanova et al., 1990). This result indicates a close coupling between basolateral and apical sorting mechanisms and raises the possibility that reductions in basolateral retrieval may be sufficient in themselves to cause increased apical transcytosis. Similar increases in apical traffic after reductions in the efficiency of basolateral sorting have been shown for receptors other than pIgR (Mellman, 1997) including TR (Odorizzi et al., 1996; Futter et al., 1998) a receptor that carries no known apical targeting information. Taking these observations on pIgR trafficking signals together with the results obtained in the present morphological studies suggests a system in which (a) dIgA/pIgR internalize and become distributed throughout the endosome along with internalized TR and EGFR; (b) EGFR become concentrated within maturing MVB whilst TR and pIgR are retrieved; and (c) phosphorylated dIgA/pIgR, inhibited from recycling, accumulate in the endosome and induce tubulation.

We show that after the internalization of dIgA/pIgR complexes, endosome vacuoles tubulate by a microtubule-

dependent mechanism and in polarized cells we presume that this results in the tubules extending into the apical cytoplasm. The presence of TR within these tubules suggests that the entry of trafficking proteins other than pIgR is not dependent upon the possession of an apical-targeting signal. However, as our recent studies on TR processing in MDCK suggest (Futter et al., 1998), trafficking proteins with basolateral signals are removed from MDCK endosomes by clathrin/AP1-sorting mechanisms and the distributions of clathrin lattices we have observed in the present study suggest that these mechanisms operate throughout the length of the transcytotic pathway from the 0.1–0.3  $\mu\text{m}$  vacuoles to the fragmenting dIgA-induced tubules. Indeed, the distribution of clathrin lattices on tubule fragments indicates that TR retrieval participates directly in the formation cup-shaped vesicles.

The release of  $^{125}\text{I}$ -Tf into the apical medium from polarized monolayers and the presence of TR within cup-shaped vesicles suggests that in the pIgR/TR expression system we have used, trafficking proteins lacking apical signals can travel the full length of the apical transcytotic pathway. It is in keeping with the data noted above which suggest that an increase in apical traffic along this pathway is often a direct reflection of the inability of basolateral retrieval mechanisms to completely clear the pathway. Thus, while the significant amount of apical TR traffic observed in this MDCK cell expression system (Odorizzi et al., 1996) is probably the result of the basolateral sorting mechanism being overloaded it is also likely that under more physiological conditions TR will be so efficiently retrieved from the earliest stages of the transcytotic pathway that they will not gain access to the dIgA-induced elements.

Our inability to identify a discrete packaging site where a local concentration of dIgA/pIgR complexes develops suggests that occupied pIgR also accumulate in cup-shaped vesicles because they escape the basolateral retrieval mechanism. However, in this case selective accumulation probably arises because dIgA/pIgR complexes become phosphorylated and, unlike TR, are unable to recycle via the clathrin-coated buds from the fragmenting tubules. This kind of sorting process, which involves the retention of one receptor subset within a forming vesicle/vacuole whilst recycling receptors (like TR) are retrieved, allows two opposing selection mechanisms to work in concert. In this respect, it is similar to the differential sorting which is thought to operate during the maturation of MVBs (Futter et al., 1996). Sorting processes operating on pathways to apical surfaces, like those en route to the lysosome, thus appear to be designed to achieve very efficient separations, more stringent than are possible in the single-step packaging of coated vesicles.

Packaging into cup-shaped vesicles may not depend entirely upon the inability of dIgA/pIgR to recycle because they could also carry apical signals that play a retention role. However, candidate signals for this purpose have not yet been identified in pIgR. It is of interest in this context that a segment has been identified within the pIgR cytoplasmic domain which, if deleted, significantly reduces apical transcytosis (Bomsel and Mostov, 1991). However, since the removal of this signal results in pIgR degradation it is more likely to operate at an earlier stage in the pathway, i.e., during tubulation or MVB maturation.

### *Sorting Endosome Vacuoles*

The microscopical results supported by the DAB cross-linking show that after being loaded for 60 min at 20°C the majority of endosomal vacuoles contain pIgR, TR, and EGFR. The colocalizations seen at 20°C are likely to be much more extensive than those that exist at 37°C because recycling and transcytosis of the internalized receptors are much reduced at this lower temperature. Incubating with tracers at 20°C allows, nevertheless, for the endosome to be preloaded and for sorting processes (such as the transfer of EGFR to the lysosome and the packaging of pIgR into vesicles) which proceed rapidly at 37°C, to be demonstrated by the temperature shift.

Previous published studies have established that tracers internalized by receptor-mediated endocytosis via coated pits enter a common pool within sorting endosome vacuoles (usually identifiable as MVB) (Geuze et al., 1983; Hopkins et al., 1990) and that they are then separated by a process of iterative sorting which transports them either to the lysosome for degradation or recycles them to the cell surface (Dunn et al., 1989; Gruenberg and Maxfield, 1995). Similar iterative mechanisms are presumably responsible for the differential processing of the radiolabeled Tf, dIgA, and EGF we have observed in the interconnected vacuoles of MDCK cells at 37°C. Previous EM studies of the sorting of TR from EGFR in the MVB of unpolarized cells (Haigler et al., 1979; Hopkins et al., 1990) showed that upon shifting to 37°C EGFR are removed to small vesicles in the vacuole lumen, whereas TR are retrieved to surrounding endosomal tubules and more recent EM studies (Futter et al., 1997) have shown this to be a gradual maturation process that produces free 0.1–0.3- $\mu\text{m}$ -diam vacuoles that then fuse with lysosomes. In MDCK cells MVB that contain EGFR and lack TR and pIgR only develop on transfer to 37°C, indicating that similar maturation processes take place in polarized cells. After preloading at 20°C and then shifting to 37°C the negligible amount of preloaded  $^{125}\text{I}$ -EGF transcytosed to the apical medium coupled with the low levels of  $^{125}\text{I}$ -dIgA and  $^{125}\text{I}$ -Tf that become degraded, relative to  $^{125}\text{I}$ -EGF, directly demonstrate the efficiency of the sorting mechanisms that operate within the MDCK endosome when MVB maturation is allowed to proceed.

### *Tubules and Tubule Formation*

Tubules have been previously identified on the apical transcytotic pathway followed by pIgR in MDCK cells (Apodaca et al., 1994) and in hepatocytes (Hemery et al., 1996). Narrow tubules also exist in MDCK cells where TR is the only exogenous receptor expressed (Odorizzi et al., 1996) but additional 100-nm-diam tubules develop in response to dIgA only in cells that express pIgR. Discrimination between the different tubule populations is difficult, however, because our EM studies show frequent continuities between them and both can be loaded with dIgA-HRP and Tf-HRP.

The 100-nm-diam dIgA-induced tubules are presumably the same as those shown to contain pIgR in an earlier study by Apodaca and colleagues that were also orientated towards centrioles (Apodaca et al., 1994). In our earlier study on MDCK expressing TR (Odorizzi et al., 1996),

similar pericentriolar concentrations of endosome tubules could not be found and in the present study pericentriolar accumulations of tubules were observed only after dIgA had induced tubulation. Our observations thus suggest that the Tf-containing tubules in the apical cytoplasm of polarized MDCK cells have a dIgA-related function and argue against them being the equivalent of the stable, signal-independent, recycling compartments previously identified in the pericentriolar areas of unpolarized cells (Hopkins, 1983; Yamashiro and Maxfield, 1984; Gruenberg and Maxfield, 1995).

The apical location and the accessibility of cup-shaped vesicles to basolateral tracers on transfer from 20° to 37°C suggests that they probably correspond to the “apical recycling endosome compartment” described in polarized MDCK cells (Apodaca et al., 1994; Barroso and Sztul 1994) and shown to release internalized pIgR tracers onto the apical surface in response to a variety of secretagogues (Mostov et al., 1995; Cardone et al., 1996). The apical recycling compartment has also been shown to be accessible to tracers introduced from the apical surface (Zacchi et al., 1998) a finding which can be explained by early observations on polarized Caco-2 cells which also showed that endosomes loaded basolaterally can be accessed by receptor-bound tracers applied apically (Hughson and Hopkins, 1990; Knight et al., 1995). It is also in keeping with the more recent observations on polarized monolayers of MDCK (Odorizzi et al., 1996) that showed their endosomes to be extensively interconnected and accessible from both surfaces.

### **The Relationship between Cup-shaped Vesicles and Other Exocytotic Vesicles**

Our results suggest that a maturation process involving the retrieval of recycling receptors via clathrin/AP 1-coated buds produces the apical, cup-shaped vesicles induced by dIgA/pIgR transcytosis. There are clear parallels between the process we have observed and those which give rise to mature secretory granules in regulated secretory pathways (Klumperman et al., 1998). However, in the transcytotic pathway it is clear that these apical vesicles arise from a TR-containing (i.e., “early”) endosome compartment and there is no evidence from our studies that either internalized dIgA or TR (Futter et al., 1998) pass through *trans*-Golgi elements or any other segment of the secretory pathways described from exocrine cells. In this respect, and together with the possibility that their exocytosis can be stimulated, the formation of transcytotic cup-shaped vesicles has features that make it closely comparable with synaptic vesicle biogenesis (Clift-O’Grady et al., 1990; Cameron et al., 1991).

This work was supported by a program grant from the Medical Research Council to C.R. Hopkins (G8417672) and by a grant from the National Institutes of Health to I.S. Trowbridge (DK-5082S).

Received for publication 1 May 1998 and in revised form 29 July 1998.

### **References**

Apodaca, G., L.A. Katz, and K.E. Mostov. 1994. Receptor-mediated transcytosis of IgA in MDCK cells is via apical recycling endosomes. *J. Cell Biol.* 125: 67–86.  
Aroeti, G., P.A. Kosen, I.D. Kuntz, F.E. Cohen, and K.E. Mostov. 1993. Muta-

tional and secondary structural analysis of the basolateral sorting signal of the polymeric immunoglobulin receptor. *J. Cell Biol.* 123:1149–1160.  
Barroso, M., and E.J. Sztul. 1994. Basolateral to apical transcytosis in polarized cells is indirect and involves BFA and trimeric G protein sensitive passage through the apical endosome. *J. Cell Biol.* 124:83–100.  
Bates, P., J.A.T. Young, and H.E. Varmus. 1993. A receptor for subgroup A Rous sarcoma virus is related to the low density lipoprotein receptor. *Cell.* 74:1043–1051.  
Bomsel, M., and K. Mostov. 1991. Sorting of plasma membrane proteins in epithelial cells. *Curr. Opin. Cell Biol.* 3:647–653.  
Cameron, P.L., T.C. Sudhof, R. Jahn, and C.P. De. 1991. Colocalization of synaptophysin with transferrin receptors: implications for synaptic vesicle biogenesis. *J. Cell Biol.* 115:151–164.  
Cardone, M.H., B.L. Smith, P.A. Mennitt, D. Mochley-Rosen, R.B. Silver, and K.E. Mostov. 1996. Signal transduction by the polymeric immunoglobulin receptor suggests a role in regulation of receptor transcytosis. *J. Cell Biol.* 133:997–1005.  
Casanova, J.E., P.P. Breitfeld, S.A. Ross, and K.E. Mostov. 1990. Phosphorylation of the polymeric immunoglobulin receptor required for its efficient transcytosis. *Science.* 245:742–745.  
Casanova, J.E., G. Apodaca, and K.E. Mostov. 1991. An autonomous signal for basolateral sorting in the cytoplasmic domain of the polymeric immunoglobulin receptor. *Cell.* 66:65–75.  
Clift-O’Grady, L., A.D. Linstedt, A.W. Lowe, E. Grote, and R.B. Kelly. 1990. Biogenesis of synaptic vesicle-like structures in a pheochromocytoma cell line PC-12. *J. Cell Biol.* 110:1693–1703.  
Courtroy, P.J., J. Quintart, and P. Baudhuin. 1984. Shift of equilibrium density induced by 3,2’-diaminobenzidine cytochemistry: a new procedure for the analysis and purification of peroxidase-containing organelles. *J. Cell Biol.* 98: 870–876.  
Dunn, K.W., T.E. McGraw, and F.R. Maxfield. 1989. Iterative fractionation of recycling receptors from lysosomally destined ligands in an early sorting endosome. *J. Cell Biol.* 109:3303–3314.  
Futter, C.E., A. Pearce, L. Hewlett, and C.R. Hopkins. 1996. Multivesicular endosomes containing internalized EGF–EGF receptor complexes mature and then fuse directly with lysosomes. *J. Cell Biol.* 132:1011–1023.  
Futter, C., A. Gibson, E. Allchin, S. Maxwell, I.S. Trowbridge, D. Domingo, and C.R. Hopkins. 1998. In polarized MDCK cells basolateral vesicles arise from clathrin- $\gamma$ -adaptin-coated domains on endosomal tubules. *J. Cell Biol.* 141:611–623.  
Geuze, H.J., J.W. Slot, G.J. Strous, and A.L. Schwartz. 1983. The pathway of the asialoglycoprotein-ligand during receptor-mediated endocytosis: a morphological study with colloidal gold/ligand in the human hepatoma cell line, Hep G2. *Eur. J. Cell Biol.* 32:38–44.  
Gruenberg, J., and F.R. Maxfield. 1995. Membrane transport in the endocytic pathway. *Curr. Opin. Cell Biol.* 7:552–563.  
Haigler, H.T., J.A. McKanna, and S.J. Cohen. 1979. Rapid stimulation of pinocytosis in human carcinoma cells A-431 by epidermal growth factor. *J. Cell Biol.* 81:382–395.  
Hemery, I., A.-M. Durand-Schneider, G. Feldmann, J.-P. Vaermann, and M. Maurice. 1996. The transcytotic pathway of an apical plasma membrane protein (B10) in hepatocytes is similar to that of IgA and occurs via a tubular pericentriolar compartment. *J. Cell Science.* 109:1215–1227.  
Hirt, R.P., G. Hughes, S. Frutiger, P. Michetti, C. Perregaux, O. Poulain-Godefroy, O. Jeanguenet, M. Neutraand, and J.-P. Kraehenbuhl. 1993. Transcytosis of the polymeric Ig receptor requires phosphorylation of serine 664 in the absence but not the presence of dimeric IgA. *Cell.* 74:245–256.  
Hopkins, C.R. 1985. The appearance and internalization of transferrin receptors at the margins of spreading human tumor cells. *Cell.* 40:199–208.  
Hopkins, C.R., A. Gibson, M. Shipman, and K. Miller. 1990. Movement of internalized ligand-receptor complexes along a continuous endosomal reticulum. *Nature.* 346:335–339.  
Hughson, E.J., and C.R. Hopkins. 1990. Endocytic pathways in polarized Caco-2 cells: identification of an endosomal compartment accessible from both apical and basolateral surfaces. *J. Cell Biol.* 110:337–348.  
Hunziker, W., P. Male, and I. Mellman. 1990. Differential microtubule requirements for transcytosis in MDCK cells. *EMBO (Eur. Mol. Biol. Organ.) J.* 11: 2515–2525.  
Klumperman, J., R. Kuliawat, J. Griffith, H. Geuze, and P. Arvan. 1998. Mannose 6-phosphate receptors are sorted from immature secretory granules via adaptor protein AP-1, clathrin and syntaxin 6-positive vesicles. *J. Cell Biol.* 141:359–371.  
Knight, A., E. Hughson, C.R. Hopkins, and D.F. Cutler. 1995. Membrane protein trafficking through the common apical endosome compartment of polarized Caco-2 cells. *Mol. Biol. Cell.* 6:597–610.  
Mellman, I. 1996. Endocytosis and molecular sorting. *Annu. Rev. Cell Dev. Biol.* 12:575–625.  
Mostov, K.E., and N.E. Simister. 1985. Transcytosis. *Cell.* 43:389–390.  
Mostov, K., G. Apodaca, B. Aroeti, and C.J. Okamoto. 1992. Plasma membrane protein sorting in polarised epithelial cells. *J. Cell Biol.* 116:577–583.  
Mostov, K.E., Y. Altschuler, S.J. Chapin, C. Enrich, S.H. Low, F. Luton, J. Richman-Eisenstat, K.L. Singer, K. Tang, and T. Weimbs. 1995. Regulation of protein traffic in polarised epithelial cells: the polymeric immunoglobulin receptor involved in transcytosis. *Cell.* 64:81–89.  
Odorizzi, G., and I.S. Trowbridge. 1994. Recombinant Rous sarcoma virus vec-

- tors for avian cells. *Methods Cell Biol.* 43:79–97.
- Odorizzi, G., A. Pearse, D. Domingo, I.S. Trowbridge, and C.R. Hopkins. 1996. Apical and basolateral endosomes of MDCK cells are interconnected and contain a polarized sorting mechanism. *J. Cell Biol.* 135:139–152.
- Okamoto, C.T., P. S-Shia, C. Bird, K.E. Mostov, and M.G. Roth. 1992. The cytoplasmic domain of the polymeric immunoglobulin receptor contains two internalization signals that are distinct from its basolateral sorting signal. *J. Biol. Chem.* 267:9925–9932.
- Rodriguez-Boulan, E., and S.K. Powell. 1992. Polarity of epithelial and neuronal cells. *Annu. Rev. Cell Biol.* 8:395–427.
- Schaerer, E., M.R. Neutra, and J.-P. Kraehenbuhl. 1991. Molecular and cellular mechanisms involved in transepithelial transport. *J. Memb. Biol.* 123:93–103.
- Simpson, F., A.A. Peden, L. Christopoulou, and M.S. Robinson. 1997. Characterization of the adaptor-related protein complex, AP-3. *J. Cell Biol.* 137:835–845.
- Slot, J.W., and H.J. Geuze. 1985. A new method of preparing gold probes for multiple labelling cytochemistry. *Eur. J. Cell Biol.* 38:87–93.
- Song, W., M. Bomsel, J. Casanova, J.-P. Vaerman, and K.E. Mostov. 1994. Stimulation of transcytosis of the polymeric immunoglobulin receptor by dimeric IgA. *Proc. Natl. Acad. Sci. USA.* 91:163–166.
- Stoorvogel, W., V. Oorschot, and H.J. Geuze. 1996. A novel class of clathrin-coated vesicles budding from endosomes. *J. Cell Biol.* 132:21–23.
- Sztul, E., A. Kaplin, L. Saucan, and G. Palade. 1991. Protein traffic between distinct plasma membrane domains: isolation and characterization of a vesicular carriers model. *Cold Spr. Harb. Symp. Quant. Biol.* 60:775–781.
- Trowbridge, I.S., J.F. Callawn, and C.R. Hopkins. 1993. Signal-dependent membrane protein trafficking in the endocytic pathway. *Annu. Rev. Cell Biol.* 9:129–161.
- Weibel, E.R. 1979. Stereological Methods. In *Practical Methods for Biological Morphometry*. Vol 1. Academic Press, London, UK. 371–380.
- White, S., K. Miller, C.R. Hopkins, and I.S. Trowbridge. 1992. Monoclonal antibodies against defined epitopes of the human transferrin receptor cytoplasmic tail. *Biochim. Biophys. Acta.* 1136:28–34.
- Yamashiro, D., B. Tycko, S. Fluss, and F.R. Maxfield. 1984. Segregation of transferrin to a mildly acidic (pH 6.5) para-Golgi compartment in the recycling pathway. *Cell.* 37:789–800.
- Zacchi, P., H. Stenmark, R.G. Parton, D. Orioli, F. Lim, A. Giner, I. Mellman, M. Zerial, and C. Murphy. 1998. Rab17 regulates trafficking through apical recycling endosomes in polarized epithelial cells. *J. Cell Biol.* 140:1039–1053.